Stem Cells, 2023, **41**, 354–367
https://doi.org/10.1093/stmcls/sxad008
Advance access publication 30 January 2023
Original Research

FAM122A Is Required for Mesendodermal and Cardiac Differentiation of Embryonic Stem Cells

Yun-Sheng Yang[1], Man-Hua Liu[1], Zhao-Wen Yan[1], Guo-Qiang Chen[*,1], Ying Huang[*,1]

[1]Department of Pathophysiology, Key Laboratory of Cell Differentiation and Apoptosis of Chinese Ministry of Education and Chinese Academy of Medical Sciences Research Unit (2019RU043, Stress and Tumor), Shanghai Jiao Tong University School of Medicine (SJTU-SM), Shanghai, People's Republic of China

[*]Corresponding author: Ying Huang, Department of Pathophysiology, Shanghai Jiao Tong University School of Medicine, 280, Chong-qing South Road, Shanghai 200025, People's Republic of China. Tel: +86 21 64154900; Fax: +86 21 64154900; Email: huangying@shsmu.edu.cn; or, Guo-Qiang Chen, Department of Pathophysiology, Shanghai Jiao Tong University School of Medicine, 280, Chong-qing South Road, Shanghai 200025, People's Republic of China. Tel: +86 21 64154900; Fax: +86 21 64154900; Email: chengq@shsmu.edu.cn

Abstract

Mesendodermal specification and cardiac differentiation are key issues for developmental biology and heart regeneration medicine. Previously, we demonstrated that FAM122A, a highly conserved housekeeping gene, is an endogenous inhibitor of protein phosphatase 2A (PP2A) and participates in multifaceted physiological and pathological processes. However, the in vivo function of FAM122A is largely unknown. In this study, we observed that *Fam122* deletion resulted in embryonic lethality with severe defects of cardiovascular developments and significantly attenuated cardiac functions in conditional cardiac-specific knockout mice. More importantly, *Fam122a* deficiency impaired mesendodermal specification and cardiac differentiation from mouse embryonic stem cells but showed no influence on pluripotent identity. Mechanical investigation revealed that the impaired differentiation potential was caused by the dysregulation of histone modification and Wnt and Hippo signaling pathways through modulation of PP2A activity. These findings suggest that FAM122A is a novel and critical regulator in mesendodermal specification and cardiac differentiation. This research not only significantly extends our understanding of the regulatory network of mesendodermal/cardiac differentiation but also proposes the potential significance of FAM122A in cardiac regeneration.

Key words: FAM122A; mESCs; mesendoderm; PP2A; cardiac differentiation.

Graphical Abstract

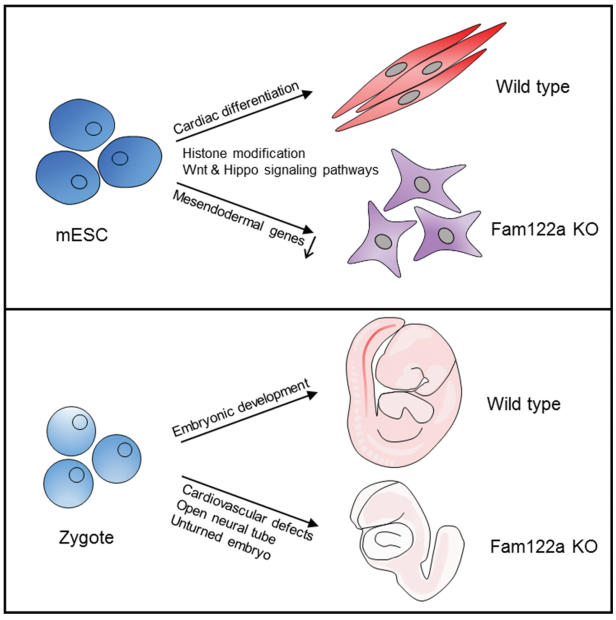

This study discusses the emerging role of FAM122A in mesendodermal specification and cardiac differentiation, as well as mouse embryonic development. *Fam122a* deletion results in impaired mesendodermal and cardiac differentiation. The impaired differentiation is caused by the dysregulation of histone modification and Wnt and Hippo signaling pathways, which are important for normal mesendodermal/cardiac differentiation.

Received: 20 August 2022; Accepted: 16 December 2022.

Significance Statement

Mesendodermal specification and cardiac differentiation are key issues for developmental biology and heart regeneration medicine. This study demonstrated for the first time that FAM122A, which was previously identified as a protein phosphatase 2A (PP2A) inhibitor, is a novel and critical regulator in mesendodermal/cardiac differentiation and early cardiac development. Impaired differentiation of *Fam122a* deletion was associated with the dysregulation of histone modification and Wnt and Hippo signaling pathways. These results reveal the essential role of FAM122A in cardiac differentiation and the possible potential significance in cardiac regeneration and linkage of PP2A and 3-germ layer development, which have not been characterized previously.

Introduction

Heart is the first and functional organ during embryonic development dedicated to the transportation of oxygen, nutrients, and wastes to and from the embryos, and it is vital to embryo survival. Cardiogenesis is a very complicated process involving cardiomyocyte (CM) differentiation, non-CM lineage specification, and a series of morphogenetic events.[1,2] Briefly, it comprises pluripotent epiblast from inner cell mass, 3–germ layer cells or gastrulation stage (endoderm, mesoderm, and ectoderm), and subsequent differentiation along with cardiac mesoderm and cardiac progenitor specification, which includes myocardial and endocardial cells and smooth muscle cells. The cardiac precursor cells (CPCs) further migrate and fuse at the embryonic midline to form the linear primary heart tube and develop into functionally matured cells, finally transforming into a looped, multichambered, valved pump organ in a proper morphogenetic patterning.[1,3]

Mesendoderm (ME), referring to the primitive streak during gastrulation, has the potential to differentiate into mesoderm and endoderm, which further develop into a series of mesoderm and endoderm tissues, respectively, and organs, such as embryonic heart, vasculature, hematological system, muscle, lung, and liver.[4] Thus, ME specification is an important and intermediate phase for heart development from pluripotent epiblast or embryonic stem (ES) cells during early embryonic development. ME formation is highly organized and spatiotemporally controlled via coordinated networks, including a number of essential transcription factors (TFs) specific for ME, epigenetic regulators, chromatin remodeling factors, and signaling pathways.[5-7] However, the dynamic regulation and precise mechanism of ME specification are not well understood.[7] Eomesodermin (*Eomes*) and brachyury (*T*), which are T-box TFs, are essential for ME specification between embryonic day (E) 6.5 and 7.5 in the mouse, and disruption of either one results in defects in cardiac mesoderm differentiation and embryonic lethality due to gastrulation defects.[8-10] *Eomes* expression marks the earliest cardiac mesoderm and dictates the formation of cardiac precursors through regulating the master TF mesoderm posterior 1 (*Mesp1*).[11] These critical TF expressions in ME are dependent on the activation of several important signaling pathways, including Wnt and transforming growth factor-β (TGF-β) signaling pathways.[6,10] Wnt ligands bind to Frizzled receptors to activate β-catenin, which directly binds the upstream regulatory regions in most ME genes, including *T*, *Eomes*, and *Mixl1*.[12,13] Besides Wnt signaling, TGF-β family member Nodal binds activin receptor to drive ME specification by Smad TF family members.[14,15] β-catenin and Smad2/3 TFs collaboratively activate ME genes.[5,16] In addition, Hippo signaling has recently been found to be involved in the modulation of this transcriptional program as a negative regulator.[17] Upstream signals phosphorylate Yes-associated protein (YAP)/transcriptional co-activator with PDZ(PSD-95/Dlg/ZO-1)-binding motif (TAZ), leading to its restriction in cytoplasm by 14-3-3 binding and further proteasomal degradation. Non-phosphorylated YAP/TAZ translocates to the nucleus and binds with TEA domain transcription factors, which triggers the transcriptional activation of target genes.[18] YAP exerts transcriptional repression in the regulation of ME gene by suppressing *Wnt3*.[17] These signaling pathways and TFs have a crosstalk with histone modifications and chromatin remodeling to coordinately regulate ME specification and myocardial differentiation.[5,6]

Family with sequence similarity 122A (FAM122A) was first identified as an endogenous inhibitor of protein phosphatase 2A (PP2A),[19,20] and its inhibitory effect in the regulation of replication stress was further confirmed by Li et al.[21] Later, FAM122A was renamed as PP2A-Aα (PPP2R1A) and -B55A (PPP2R2A) interacting phosphatase regulator 1 (PABIR1) in human. *FAM122A*, a highly conserved housekeeping gene, localizes on chromosome 9q21.1 within the first intron of *phosphatidylinositol 4-phosphate 5-kinase* (*PIP5K1B)* gene and encodes 287 amino acids. FAM122A knockout (KO) suppresses the growth of hepatocellular carcinoma cells and acute myeloid leukemia cells in vitro and in vivo, with independence or dependence of PP2A inhibitory activity.[22,23] In addition, FAM122A is essential for maintaining the self-renewal capability of hematological stem cells[24] and required for the differentiation of erythroid cells;[25] FAM122A also contributes to the maintenance of DNA stability in malignant tumor cells.[26] These studies suggest that FAM122A has multifaceted functions under physiological or pathological circumstances. However, the in vivo function of FAM122A remains unknown.

In this study, we used *Fam122a* KO mice, conditional cardiac-specific *Fam122a* KO mice, and mouse ES cells (mESCs) to address the role of FAM122A in embryonic development and CM differentiation. We showed that *Fam122a* deficiency led to early embryonic lethality with severe defects of heart development, and impaired cardiac function was found in conditional KO mice. More importantly, we observed that FAM122A KO significantly disrupted ME specification and myocardial differentiation, which is cooperatively dysregulated by histone modifications and Wnt and Hippo signaling pathways.

Materials and Methods

Mouse Use and Maintenance

Fam122a KO mice were produced by East China Normal University (C57BL/6 and 129/SvJ mixed background). *Fam122a* gene was inactivated by targeting the unique exon. Supplementary Fig. S1A shows the schematics of targeted disruption of *Fam122a*. *Fam122a* floxed mice were produced by Shanghai Renyuan Biotechnology as described previously.[24] *Myh6*-Cre mice were purchased from Shanghai Model

Organisms Center, Inc., and *Nkx2-5*-Cre mice were bought from Jiangsu Gempharmatech Biotechnology. *Fam122a* conditional KO mice were on a C57BL/6 background. All animal experiments were carried out as approved by the Laboratory Animal Resource Center of Shanghai JiaoTong University School of Medicine.

Embryo Collection and Whole-Mount In Situ Hybridization

Whole-mount in situ hybridization assay was performed as described previously.[27] For embryo collection, mice were maintained on a 12/12 h light/dark cycle. After mating, the morning of appearance of a vaginal plug was designated as embryonic day 0.5 (E0.5). At the determined embryonic day, mouse embryos were dissected in cold diethyl pyrocarbonate-treated phosphate-buffered saline + 0.1% Tween 20 (PBST). Then, the embryos were fixed with 4% paraformaldehyde (PFA) in PBST at 4 °C and dehydrated stepwise through a methanol/PBST series (25%, 50%, 75%, and 100% methanol). Embryos can be stored at −20 °C in 100% methanol. RNA probes were generated by in vitro transcription from linearized plasmids using a DIG RNA Labelling Kit (SP6/T7). Rehydrated embryos were incubated in 4:1 PBST:30% H_2O_2 for 1 h on ice and digested with 1 mL 10 μg mL^{-1} proteinase K in PBST in a 25 °C water bath. Digested embryos were fixed for 20 minutes at room temperature in 4% PFA/PBST and 0.2% glutaraldehyde and hybridized overnight at 65 °C. Embryos were pre-blocked in 0.5 mL Tris-buffered saline with 0.1% Tween 20 (TBST) + 10% heat-treated sheep serum and incubated with 1:2500 dilution of anti-DIG-alkaline phosphatase (AP) antibody at 4 °C overnight.

Then, the embryos were stained with BM Purple AP substrate, and the reaction was stopped by washing with 5 mM ethylenediaminetetraacetic acid (EDTA) in PBST. Embryos can be re-fixed and stored in 4% PFA/PBST.

Hematoxylin and Eosin Staining

Embryos were fixed in Bouin's solution, and hearts from *Fam122a* conditional KO mice were fixed in 4% PFA and then processed for paraffin embedding. Sections (3.5 μm thick) were cut, dewaxed, rehydrated, and stained with hematoxylin and eosin (HE) solutions.

Genotyping

Mice were genotyped using a 2 mm piece of the toe or tail tip. The tissues were incubated overnight at 55 °C in 200 μL lysis buffer (50 mM NaCl, 10 mM Tris-HCl [pH 8.0], 5 mM EDTA, and 0.1% sodium dodecyl sulphate [SDS]) containing 75 μg proteinase K. The lysate can be used for polymerase chain reaction (PCR) directly or precipitated with isopropanol and dissolved in Tris-EDTA (TE) buffer. For a single embryo or yolk sac, DNA was extracted by KAPA Express Extract Kit following the manufacturer's instruction. PCR primers are listed in Supplementary Table S1.

ESC Culture

R1/E (purchased from Cell Bank of Chinese Academy of Sciences) and TC1 (a gift from J. Kang)[28] cells were maintained in Dulbecco's Modified Eagle Medium (Basal Media) supplemented with 15% fetal bovine serum (Gibco), 1 × non-essential amino acids (Gibco), 1 × GlutaMAX (Gibco), 1 × sodium pyruvate (Gibco), 0.1 mM β-mercaptoethanol (Sigma), 1000 U mL^{-1} leukemia inhibitory factor (LIF) (Millipore), 100 U mL^{-1} penicillin, and 100 μg mL^{-1} streptomycin on mitomycin C (Selleck) inactivated mouse embryonic fibroblast feeder cells under 5% CO_2 at 37 °C. ESCs were passaged every other day using 0.25% Trypsin at a split ratio of 1:5.

Generation of *Fam122a* KO mESCs

The sgRNAs targeted to the exon of *Fam122a* were inserted into the pX330 vector and are listed in Supplementary Table S1. The plasmids were electroporated into mESCs at 250 V and 500 μF in a 0.4 cm Gene Pulser cuvette (Bio-Rad). Then, mESCs were replated on feeder cells, and individual colonies were picked and expanded. The deletion of FAM122A was validated by Western blot.

AP Staining

ESC colonies were cultured on 12-well plates for 5 days, and AP staining was performed with the AP detection kit (Millipore) following the manufacturer's instructions. Briefly, the cells were fixed with 4% PFA at room temperature for 2 minutes and rinsed with TBST. Then, the cells were stained with naphthol/Fast Red Violet solution (Fast Red Violet, naphthol AS-BI phosphate solution and water at a 2:1:1 ratio) in the dark at room temperature for 15 minutes, rinsed with TBST, covered with PBS, and imaged using a scanner.

Embryonic Body Formation and Cardiac Differentiation

The cardiac muscle cell differentiation protocol was performed as described previously.[29] Briefly, mESCs were dissociated, and 300 cells in 30 μL culture medium without LIF were aggregated to form embryonic body (EB) by hanging drop for 2 days or 2.5×10^5 cell cultured with 5 mL medium in 60 mm bacterial culture dish in suspension for mass culture. EBs were harvested and transferred to 60 mm bacterial culture dish with 5 mL medium for 3 days. Then, a single EB was plated onto each well of 0.1% gelatin (Sigma)-coated 24-well microwell, and the medium was changed every other day. The beating EBs were counted, shot for videos, and used further analysis.

Immunostaining

For immunostaining, cells were fixed with 4% PFA at room temperature for 20 minutes and permeabilized with 0.1% Triton X-100 for 10 minutes. Then, the cells were blocked with 5% bovine serum albumin for 1 h and incubated with primary antibodies (anti-TNNT2, Abcam#ab8295; anti-SRY-box transcription factor 2 [SOX2], Abclonal#A0561) overnight at 4 °C and Alexa Fluor 488- or 594-conjugated secondary antibody (Abcam#ab150077, ab150116) at room temperature for 1 h. Finally, the slides were mounted in antifade mounting medium with 4′,6-diamidino-2-phenylindole (Vectorshield) and imaged using a fluorescent or confocal microscope.

For D4 EBs, cells were permeabilized with 0.5% Triton X-100 for 15 minutes and incubated with primary antibody (T, Abcam#ab209665) overnight at 4 °C.

Quantitative Reverse Transcription (qRT)-PCR

Total RNA was extracted from cells using RNAiso (Takara). A total of 2 μg RNA was removed of genomic DNA and reverse transcribed into cDNA with FastKing-RT SuperMix (Tiangen). Diluted cDNA was used in qRT–PCR reaction with PowerUp SYBR Master Mix (ABI) on an Applied Biosystems QuantStudio 5. The relative expression level was calculated

using the $2^{-\Delta\Delta Ct}$ method, and glyceraldehyde 3-phosphate dehydrogenase (*Gapdh*) gene served as the internal reference. Each experiment was performed in triplicate and repeated thrice. Supplementary Table S1 lists the primer sequences used in this study.

Western Blot

Proteins were extracted using 1 × SDS lysis buffer (50 mM Tris-HCl [pH 6.8], 100 mM DTT, 2% SDS, and 10% glycerol) and separated by SDS-polyacrylamide gel electrophoresis. Then the proteins were transferred to a nitrocellulose (NC) membrane (Millipore) and blocked with 5% skim milk in TBST at room temperature for 1 h. The membranes were incubated with primary antibody overnight at 4 °C and horseradish peroxidase (HRP)-linked secondary antibody (CST, 7074) at room temperature for 1 h. The signals were detected by reacting with chemiluminescent HRP substrate (Millipore) and visualized using a chemiluminescent detector (FUJIFILM). The primary antibodies included the following: anti-FAM122A (customized by Abclonal), anti–PIP5K1B (Abnova, H00008395-A01), HRP–conjugated anti-α-tubulin (Proteintech, HRP-66031), HRP-conjugated anti-GAPDH (Proteintech, HRP-60004), anti-octamer binding transcription factor 4 (OCT4; Abcam, ab181557), anti-SOX2 (Abcam, ab92494; Abclonal, A0561), anti-Homeobox protein NANOG (NANOG; Abcam, ab214549), anti–H3K4me3 (Abcam, ab8580), anti-H3K27me3 (Millipore, 07-449), anti-H3K27ac (Abcam, ab4729), anti-histone H3 (Abcam, ab1791), anti-p-YAP (CST, 13008), and anti-YAP (CST, 14074).

RNA-Seq Library Generation

Total RNA was isolated from mESCs at the indicated days using Trizol reagent (Thermo Fisher Scientific, 15596018) in accordance with the manufacturer's protocol. Libraries were generated using NEBNext Ultra RNA Library Prep Kit (NEB, E7490) following the manual and purified using isopycnic Ampure XP beads (Beckman Coulter, A63881). Then, the libraries were sequenced using an Illumina Novaseq 6000 instrument with 150 bp reads and paired-end parameter.

RNA-Seq Data Processing

Sequencing reads were mapped to mm10 reference genome using STAR (v.2.5.2b).[30] The transcription levels of annotated genes (FPKM, fragments per kilobase of transcript per million mapped reads) were quantified using HTSeq-count (v.0.6.0).[31] Differentially expressed gene (DEG) analysis was performed using DESeq2[32] and filtered by adjusted $P < .05$ and fold-change >2. The overlapping DEGs between Fam122a KO-1 and Fam122a KO-3 were used for Gene Ontology (GO), Kyoto Encyclopedia of Genes and Genomes (KEGG) pathway, and gene set enrichment analysis (GSEA).

Flow Cytometry Analysis

D4 EBs were disassociated with Accutase (Biolegend) and washed with PBS. Then 1 × 10^6 cells were incubated with anti–FLK-1-PE (Biolegend, 121905) and anti–PDGFR-α-APC (Biolegend, 135907) at 4 °C for 30 minutes and washed with PBS. Cells were sorted using a Beckman CytoFlex Sand analyzed with FlowJo software (v.7.6).

Chromatin Immunoprecipitation

Chromatin immunoprecipitation (ChIP) assays of mESCs and EBs were performed using a ChIP-IT Express Kit (Active Motif, 53008) following the manufacturer's instructions. Briefly, the cells were cross-linked with 1% formaldehyde at room temperature for 10 minutes and quenched with 0.25 M glycine for 5 minutes. The cell pellet was incubated in lysis buffer on ice for 30 minutes and stroked to release nuclei. Chromatin was sheared to 150-500 bp fragments with a sonicator (Qsonica Q700) in Shearing Buffer. Immunoprecipitation was performed with Protein G Magnetic Beads and primary antibodies (anti-H3K4me3, Abcam#ab8580; anti-H3K27me3, Millipore#07-449; anti-H3K27Ac, Abcam#ab4729) by rotation at 4 °C overnight. Beads were washed thrice with ChIP Buffer 1 and twice with ChIP Buffer 2. Chromatin was eluted by rotation at room temperature for 15 minutes and reversed cross-linked at 65 °C for 4 h with Reverse Cross-linking Buffer. Then, the samples were incubated with RNase A at 37 °C for 15 minutes and Proteinase K at 42 °C for 1.5 h. DNA was purified using NucleoSpin Extract II Kit (MN, 740609).

ChIP-Seq Library Generation

Libraries were generated using NEBNext Ultra DNA Library Prep Kit for Illumina (NEB, E7370L) following the manufacturer's protocol. Libraries were quantified by Qubit2.0, and the qualities were determined using Agilent 2100. Then, the libraries were sequenced using an Illumina Novaseq 6000 instrument with 150 bp reads and paired-end parameter.

ChIP-Seq Data Processing

Reads were removed with poor quality calls and mapped to the mouse mm10 reference genome using Bowtie2 (v.2.4.2).[33] Multiple mapped reads and PCR duplicates were further removed using Sambamba (v.0.6.8)[34] with the parameter: *–F* "[XS] == null and not unmapped and not duplicate". Genome coverage bigwig files were generated by deepTools (v.3.5.0)[35] bamCoverage with the parameters "--normalizeUsing RPKM --binSize 20" and visualized using IGV (v.2.9.4).[36] Heatmaps were created by deepTools computeMatrix and plot Heatmap.

Echocardiography

Echocardiography was performed using a digital small-animal ultrasound system (VisualSonics, Vevo 2100 or Vevo 3100). Male mice (12-16 weeks old) were constantly anesthetized with 2% isoflurane and placed in the supine position on a heated platform. The mouse chest skin was depilated with hair removal cream and applied with acoustic gel. Two-dimensional long- or short-axis B-Mode and M-Mode views were obtained. Ejection fraction (EF), fractional shortening (FS), cardiac output (CO), left ventricular internal diameter in systole (LVIDs), and interventricular septum (IVS) were calculated.

Statistical Analyses

Statistical analyses were performed using GraphPad Prism 6. All data in this study are presented as means ± SD from 3 independent experiments. The *P* values were calculated using unpaired 2-tailed Student's *t* test.

Data Availability

All RNA-seq and ChIP-seq data in this study have been deposited to the Gene Expression Omnibus with the accession number GSE211341.

Results

Fam122a Deletion Results in Embryonic Lethality and Defects of Cardiovascular Development

To investigate the potential function of FAM122A in vivo, we applied CRISPR/Cas9 technique to generate *Fam122a* gene KO mice (Supplementary Fig. S1A, Materials and Methods). Heterozygous *Fam122a*$^{+/-}$ mice with 29 bp deletion were intercrossed to produce *Fam122a* deletion homozygous mice (*Fam122a*$^{-/-}$). Among a cohort of 210 progenies, 69 (32.86%) were wild-type (WT) for *Fam122a*$^{+/+}$, and 141 (67.14%) were heterozygous for *Fam122a*$^{+/-}$. These data are consistent with the predicted 1:2 Mendelian ratios (Supplementary Fig. S1B) for WT over heterozygous mice. No viable homozygous *Fam122a*$^{-/-}$ mouse was obtained, which suggests that the deletion of *Fam122a* gene led to embryonic lethality.

To determine the time of embryonic lethality in *Fam122a*$^{-/-}$ mice, we extracted genomic DNA from embryos harvested at different stages in pregnant *Fam122a*$^{+/-}$ mice. PCR-based analysis was used to determine the genotype of these embryos (Supplementary Fig. S1C). Western blot further confirmed that FAM122A protein decreased in *Fam122a*$^{+/-}$ and was absent in *Fam122a*$^{-/-}$ embryos, whereas no difference was observed in the PIP5K1B protein level (Supplementary Fig. S1D), which suggests that *Fam122a* gene was successfully and specifically ablated. *Fam122a*-null embryos decreased gradually from E9.5 to 11.5 but were absent on E12.5 due to reabsorption (Supplementary Fig. S1E). *Fam122a*–null embryos on E9.5 were easily distinguished from their WT littermates by severe growth retardation and multiple structural malformations, including smaller size, open anterior neural folds, defects of somatic formation and turning, enlarged pericardial cavity or pericardial effusion, together with the absence of large vessel formation in yolk sac, the latter being signs of cardiovascular defects (Supplementary Fig. S1G). *Fam122a*-deficient embryos on E8.5 also showed partial developmental delays, such as smaller head folds and reduced extra-embryonic tissues, compared with the WT ones (Supplementary Fig. S1F). Histological analysis further confirmed the morphological findings in E9.5 *Fam122a*-deficient embryos, particular the profound cardiac abnormalities, including defects of atrial and ventricular chambers with thinner myocardial walls (Supplementary Fig. S1H). Heterozygous FAM122A$^{+/-}$ mice were normal and fertile. These results strongly suggest that the loss of *Fam122a* leads to embryonic lethality with severe defects of cardiovascular development. Thus, in this study, we mainly focused on whether FAM122A has a role in cardiac differentiation and development.

Fam122a Deletion Impairs CM Differentiation in mESCs

In situ hybridization analysis showed that *Fam122a* was expressed broadly without tissue specification and upregulated from E7.5 to E9.5 (Supplementary Fig. S2A). To evaluate the possible role of FAM122A in cardiac differentiation, we induced mESC differentiation by hanging drop EBs in LIF-free medium, which allowed the stepwise differentiation of mESCs toward the cardiogenic lineage, generating ME precursor cells (MEPCs), CPC, and ultimately differentiated CMs (Fig. 1A).[6] We found that *Fam122a* gene and protein levels declined mildly at the initial 4 days and rose rapidly after 6 days of differentiation with the upregulation of *Tnnt2* (a tropomyosin-binding subunit of cardiac troponin complex, an indicator of CMs[37]; Fig. 1B, 1C), which suggests that FAM122A may participate in the differentiation process. CRISPR/Cas9-mediated *Fam122a* KO mESCs were generated by 2 sgRNAs, designated as Fam122a KO-1 and Fam122a KO-3. Deletion of FAM122A in mESCs R1/E, which was confirmed by Western blot (Supplementary Fig. S2B), significantly reduced the percentages of beating EBs and the expressions of CPC (*Nkx2-5*, *Gata4*, *Tbx5*, and *Isl1*[38]) and CM (*Myl2*, *Myh6*, *Tnnt2*, and *α-SMA*[28]) marker genes and TNNT2 protein on day 7 (D7) and D10 of EB differentiation (Fig. 1D–1G; Supplementary Fig. S2G; videos S1–S3), although FAM122A KO did not evidently change the morphology of ESC colonies (Supplementary Fig. S2C). Similar differentiation defects were found in another *Fam122a* deletion mESC TC1 (Supplementary Fig. S3D–S3F). *Fam122a* deletion did not affect the expression levels of stem cell-correlated genes (*Oct4*, *Sox2*, and *Nanog*; Supplementary Figs. S2D, S2E, S3A–S3C) and the activity of AP[39] (Supplementary Fig. S2F). Thus, FAM122A may be essential for CM differentiation, but it shows no influence on stem cell identity.

FAM122A Regulates a Core Network of Genes that Drive Cardiac Differentiation

To further explore the mechanism of FAM122A on CM differentiation, we performed RNA sequencing for global gene expressions in WT and 2 Fam122a KO mESCs during different differentiation stages. The overlapping DEGs (2-fold cutoff) in Fam122a KO-1 and Fam122a KO-3 vs. WT totaled 1023 on D7 of differentiation, and most of them were downregulated (Fig. 2A). GO and pathway analysis showed that *Fam122a* deletion-modulated genes were mainly enriched in multicellular organismal and developmental process and different cardiomyopathies and heart functions, including dilated cardiomyopathy, hypertrophic cardiomyopathy, cardiac muscle contraction, arrhythmogenic right ventricular cardiomyopathy, and adrenergic signaling in CMs (Fig. 2B, 2C). The downregulation of multiple CPC-related genes, including several TFs, and cardiac muscle- and iron channel-related genes were observed in *Fam122a*-deleted mESCs on D7 of differentiation (Fig. 2D). Consistently, the RNA-seq result on D10 differentiation also showed that *Fam122a* deletion suppressed the terminal CM differentiation genes (Fig. 2E–2H).

In vitro cardiac differentiation, EBs in suspension formed by pluripotent ESCs may recapitulate the signaling and transcriptional events for the specification of 3-germ layers, which is mirrored in the gastrulation process in vivo.[12] Eomes, T, Mesp1, and Mixl1 are critical TFs, and depletion of these factors individually can significantly impair ME specification and cardiac differentiation.[10,11,40] Intriguingly, RNA-seq result on D4 EBs showed the reduced expression of 122 genes in Fam122a KO vs. WT, whereas 120 genes were upregulated (Fig. 3A). GO analysis further revealed that *Fam122a* deletion led to the significant downregulation of ME genes, including *T*, *Eomes*, *Mixl1*, *Wnt3*, *Gsc*, and *Foxa2* (Fig. 3B; Supplementary Fig. S3G), which was further confirmed by qPCR (Fig. 3C) and time course analysis

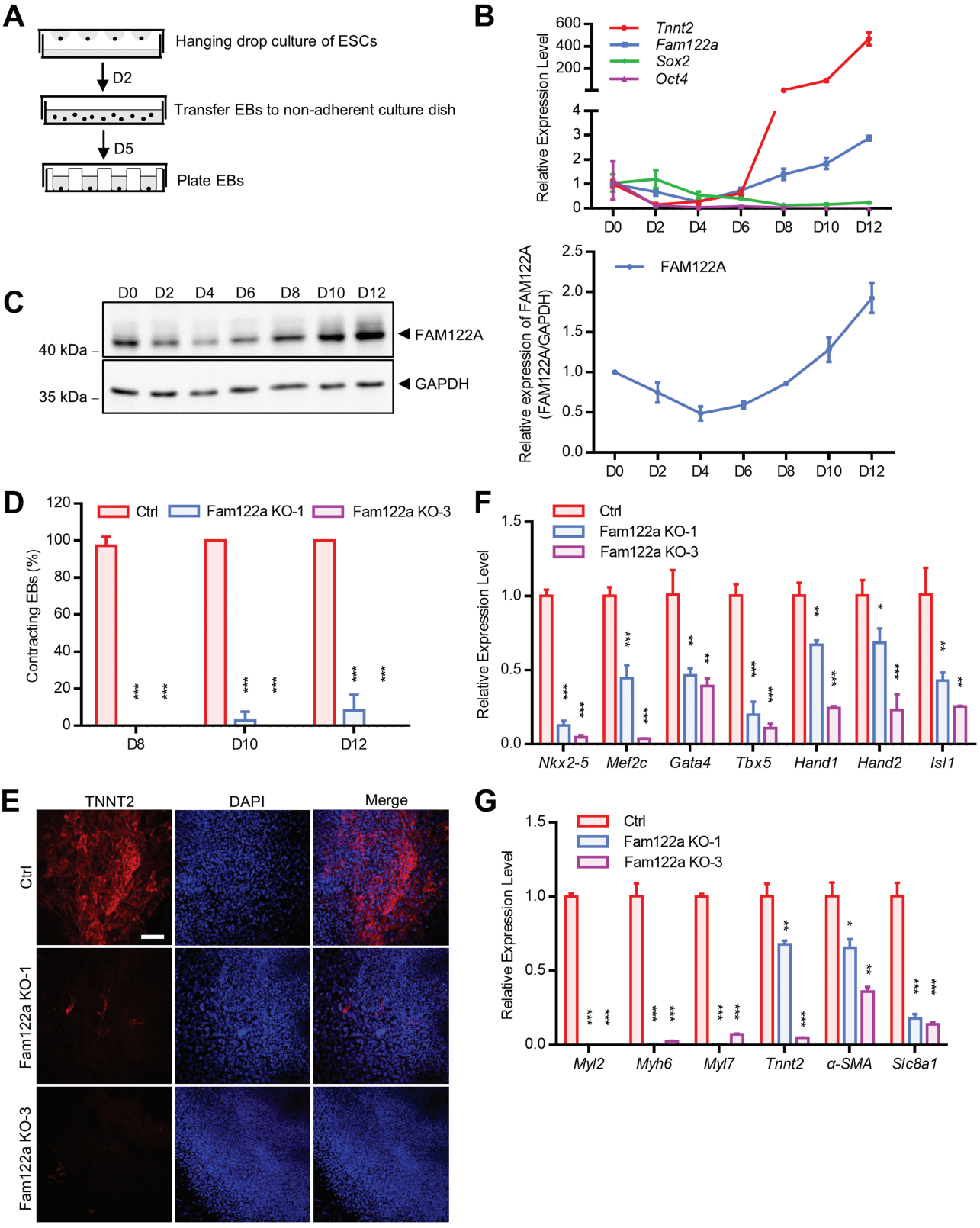

Figure 1. Cardiac differentiation defect in *Fam122a* knockout mESCs. (**A**) Schematic of mESCs differentiation assay. The mESCs are trypsinized, aggregated to EBs by hanging drop and subsequently plated to differentiation. (**B**) qRT–PCR analysis of *Tnnt2*, *Fam122a*, *Sox2*, and *Oct4* expression. (**C**) Western blot analysis of FAM122A expression during mESCs differentiation (left), and quantification of 3 experiments (right). (**D**) Percentages of contracting EBs determined from D8 to D12 of mESCs differentiation. (**E**) TNNT2 immunostaining on D10 of mESCs differentiation. Scale bar = 100 μm. (**F**) qRT-PCR analysis of cardiac progenitor marker genes on D7 of mESCs differentiation. (**G**) Expression analysis of cardiomyocyte marker genes on D10 of mESCs differentiation. In (D), (F) and (G), data represent means ± SD from $n = 3$ independent experiments, and P values were calculated by 2-tailed unpaired t test (* $P < .05$, ** $P < .01$, and *** $P < .001$).

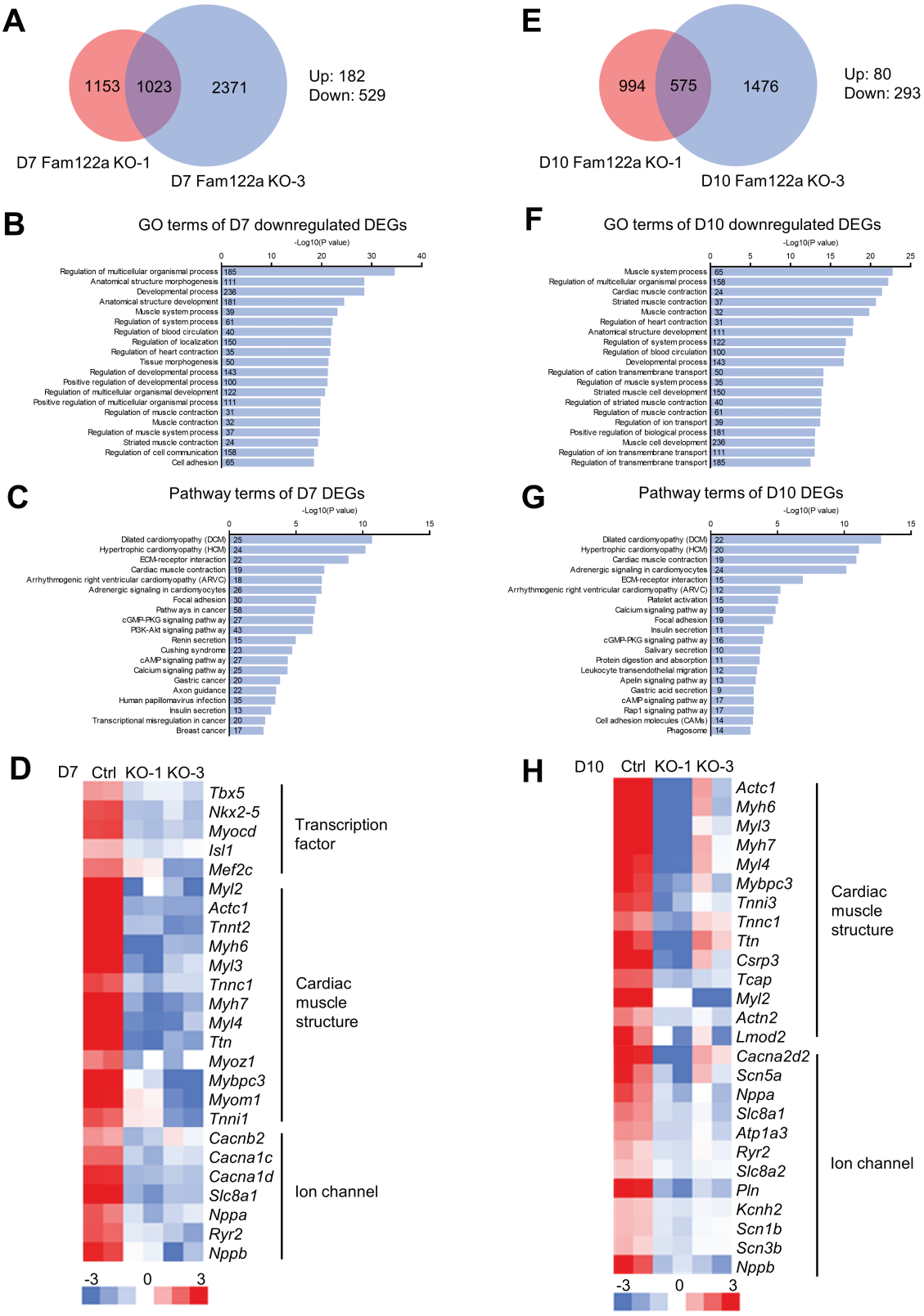

Figure 2. RNA-seq analysis of D7 and D10 *Fam122a* knockout differentiated mESCs. (**A**) Venn diagram showing the overlapped DEGs in D7 KO mESCs. (**B**) Gene ontology analysis of the D7 downregulated DEGs. (**C**) KEGG pathway analysis of the D7 DEGs. (**D**) Heatmap showing the representative D7 downregulated cardiac genes. (**E**) Venn diagram showing the overlapped DEGs in D10 KO mESCs. (**F**) Gene ontology analysis of the D10 downregulated DEGs. (**G**) KEGG pathway analysis of the D10 DEGs. (**H**) Heatmap showing the representative D10 downregulated cardiac genes. Numbers in bars show the gene numbers of the corresponding gene ontology or pathway categories (B, C, F, and G).

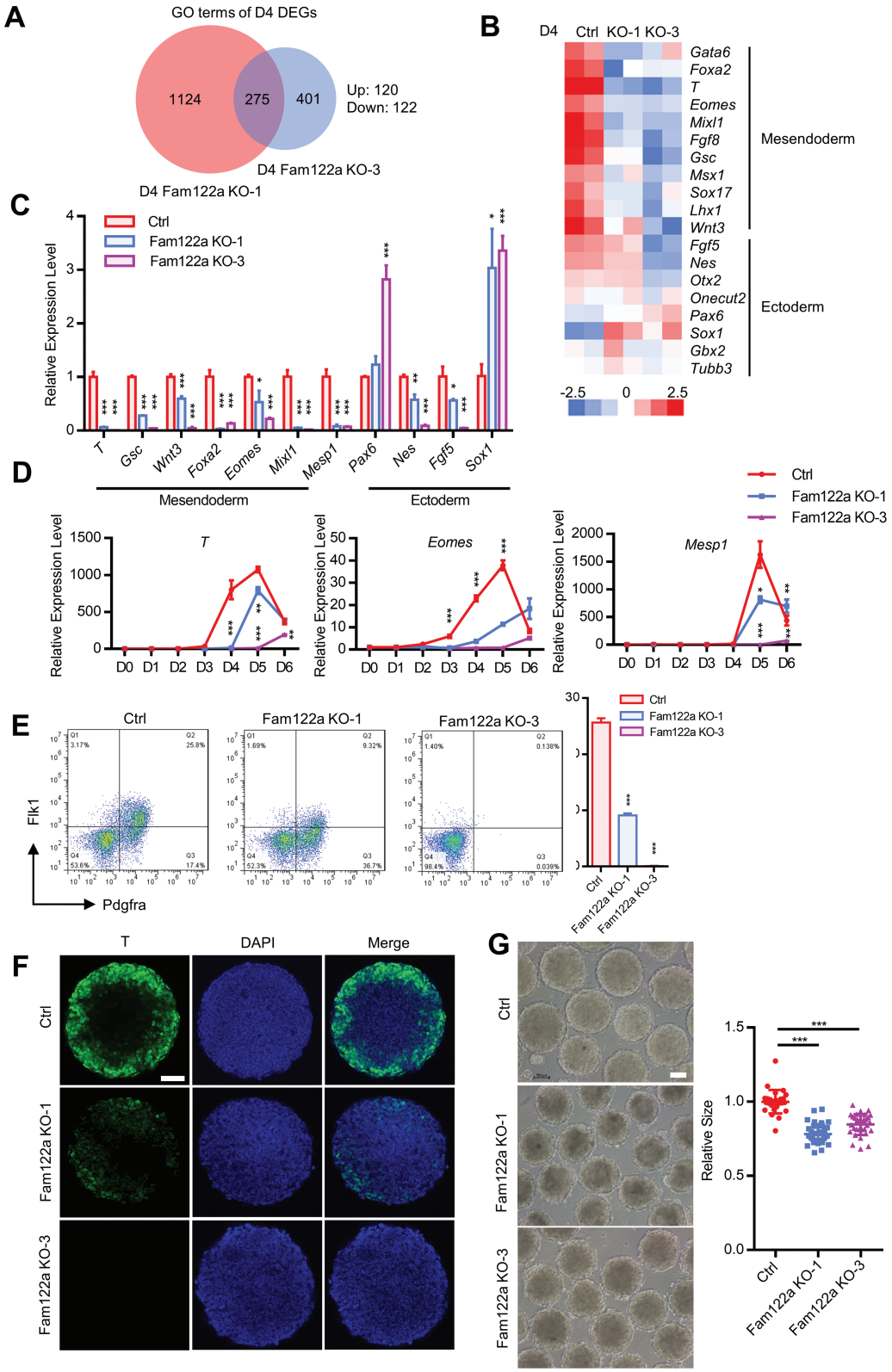

Figure 3. Mesendodermal differentiation defect in D4 *Fam122a* knockout EBs. (**A**) Venn diagram showing the overlapped RNA-seq DEGs in D4 KO EBs. (**B**) Heatmap showing the representative D4 DEGs of 3-germ layer markers. (**C**) qRT-PCR analysis of 3-germ layer marker genes on D4 of EB differentiation. (**D**) Expression analysis of *T*, *Eomes*, and *Mesp1* determined from D0 to D6 of EB differentiation. (**E**) Fluorescence-activated cell sorting (FACS) analysis of the percentage of Flk1$^+$/Pdgfra$^+$ cells differentiated from D4 EBs (left) and quantification (right). (**F**) T immunostaining of control and Fam122a KO EBs on D4. Scale bar = 50 μm. (**G**) Images of D4 EBs in control and Fam122a KO mESCs (left), and quantification of EBs size (right). Scale bar = 100 μm. In (C), (D), (E), and (G), data represent means ± SD from $n = 3$ independent experiments, and P values were calculated by 2-tailed unpaired t test (* $P < .05$, ** $P < .01$, and *** $P < .001$).

(Fig. 3D). *Fam122a* deletion also reduced the immunofluorescence staining for T protein (Fig. 3F) and the percentages of Flk1^{+}/Pdgfra^{+} cardiac MEPCs (Fig. 3E).[41] These results strongly suggest that ME differentiation was blocked in Fam122a KO mESCs. In addition, *Fam122a*-deleted mESCs demonstrated smaller sizes of EBs on D4 of differentiation (Fig. 3G). *Fam122a* deletion also reduced the expression of partial ectoderm-related genes *Nes* and *Fgf5* (Fig. 3C). Collectively, FAM122A is critical for ME specification of mESCs.

Fam122a Deletion Reduces the Binding Activities of H3K4me3 and H3K27ac on Mesendodermal Genes

Substantial ME genes were suppressed in *Fam122a* depleted mESC-formed EBs on D4, which suggests that FAM122A may directly or indirectly regulate gene expression as a TF, by modulating transcriptional activity as a cofactor or by changing the chromatin structure as a modifier. GSEA of Fam122a KO and WT mESCs showed that DEGs were significantly enriched in H3K4me2 and H3K27me3 datasets (Fig. 4A), which indicates that FAM122A may modulate histone post-translational modifications. Therefore, we performed ChIP-seqs of H3K4me3 and H3K27ac (transcriptional activation markers) and H3K27me3 (a transcriptional repression marker).[5,42] We also compared their protein levels in Fam122a KO and WT ESCs on D0 and D4 EBs. Heatmaps showed that the enrichments of H3K4me3 and H3K27ac were significantly enhanced in D4 EBs compared with D0 (Supplementary Fig. S4A–S4C), which paralleled the shift of transcriptional repression to activation following differentiation induction. *Fam122a* deletion decreased H3K4me3 binding on D0 and increased H3K27me3 binding on D4 EBs, whereas H3K27ac showed no remarkable change. The changes in binding capacity were accompanied by the increase in H3K27me3 protein in D4 EBs compared with D0, but no significant alteration was observed in H3K4me3 and H3K27ac proteins (Fig. 4B). More importantly, *Fam122a* depletion significantly decreased the occupancy of H3K4me3 and H3K27ac in the promoters of *T* and *Eomes* genes in D4 EBs but did not change the binding of H3K27me3 in these genes on D0 and D4 ESCs (Fig. 4C). The reduced H3K4me3 and H3K27ac binding on ME genes were consistent with our observation that *Fam122a* depletion disrupted ME gene expression and specification. In addition, decreased expression of ectoderm gene *Fgf5* upon *Fam122a* deletion was accompanied by reduced H3K27ac binding on its promoter in D4 EBs, whereas enhanced expression of *Sox1* was paralleled by the increased binding activity within H3K4me3 and H3K27ac loci (Supplementary Fig. S4D). These results implied that *Fam122a* deletion induces the suppression of ME genes through histone modification.

To test whether FAM122A modulates the transcriptional activity of ME genes by interacting with any essential enzymes for histone modification, we performed immunoprecipitation and mass spectrometry (IP-MS) to screen interacting protein profiles in Flag-FAM122A-overexpressing mESCs and 293T cells. However, we found no interaction of FAM122A with histone modifiers, such as methyltransferase, acetyltransferase, demethylase, or deacetylase (data not shown), which suggests that FAM122A regulating ME genes and histone modification is not directly modulated by histone modifiers.

Fam122a Deletion Aberrantly Regulates Wnt and Hippo Signaling Pathways

To further determine the underlined causes of *Fam122a* deletion impairing the ME genes and differentiation, we closely analyzed the DEGs in D4 differentiated EBs with or without *Fam122a* depletion. KEGG analysis showed that these DEGs were mainly enriched in the regulation of pluripotent stem cell fate and Wnt and Hippo signaling pathways (Fig. 4D), with both signaling pathways having an effect on histone modification.[43-46] Wnt signaling activation is critical for ME gene expression and specification,[16,47] whereas the effector of Hippo signaling YAP directly antagonizes ME gene activation as a co-repressor.[17,48] Considering that FAM122A has been identified originally as an endogenous inhibitor of PP2A, we examined the phosphorylation levels of PP2A substrates in Wnt (β-catenin and GSK-3β) and Hippo (YAP) signaling.[49-54] The results showed that the phosphorylations of YAP, β-catenin, and GSK-3β were significantly reduced in D0 Fam122a KO mESCs compared with those of WT cells (Fig. 4E). However, these effects were not significant in D4 EBs. The addition of okadaic acid (OA, a PP2A inhibitor) not only eliminated the reduced phosphorylation of YAP, β-catenin, and GSK-3β by *Fam122a* deletion but also partially rescued *Fam122a* deletion-induced decrease in the expression of ME genes (Fig. 4F, 4G).

Fam122a Depletion Impairs Cardiac Development and Function in Conditional Cardiac KO Mice

To strengthen the critical role of FAM122A in cardiac development and function, we crossed *Fam122a*$^{fl/fl}$ mice (Supplementary Fig. S5A, S5B) with *Myh6*-Cre transgenic mice[55] to generate mice where *Fam122a* is genetically and specifically inactivated in CMs of the heart tube on E8.5. Western blot confirmed the KO effect of FAM122A (Supplementary Fig. S5C), and echocardiography analysis showed that *Fam122a* deletion significantly impaired cardiac functions, as determined by the decreases in heart weight ratio, percentages of EF and FS, and stroke volume (SV) in *Myh6*-Cre *Fam122a*$^{fl/fl}$ mice compared with *Fam122a*$^{fl/fl}$ ones (Fig. 5A, 5B). Moreover, we observed that LVIDs increased, whereas IVS thickness in diastole (IVSd) and in systole (IVSs) reduced in *Myh6*-Cre *Fam122a*$^{fl/fl}$ mice (Fig. 5C, 5D). Similar effects of *Fam122a* deletion on cardiac dysfunction were found in other conditional cardiac-specific *Fam122a* KO mice (*Nkx2-5*-Cre *Fam122a*$^{fl/fl}$) by using *Nkx2-5*-Cre mice, with *Nkx2-5*-Cre-mediated recombination occurring on E7.5 cardiac progenitor cells during cardiac crescent,[56] which can elucidate the function of FAM122A during the earliest stages of cardiogenesis (Supplementary Fig. S5D–S5H). Notably, *Fam122a* deletion can significantly decrease the body and heart weights of *Nkx2-5*-Cre *Fam122a*$^{fl/fl}$ mice but not *Myh6*-Cre *Fam122a*$^{fl/fl}$ mice. Thus, *Fam122a* deletion at earlier cardiac development may result in more severe effects on heart development and function.

Discussion

ME is an important event in early embryonic development. In-depth understanding of the regulatory networks of ME specification from ESCs in vitro or pluripotent epiblast in vivo may provide important insights into early embryonic patterning and a possible guidance for ES applications in regenerative medicine, especially in heart regeneration field.[57,58]

A

GSEA geneset	Enrichment	P-value
MEISSNER_NPC_HCP_WITH_H3K4ME2_AND_H3K27ME3	0.48	0
MEISSNER_BRAIN_HCP_WITH_H3K27ME3	0.49	0.003
MIKKELSEN_NPC_HCP_WITH_H3K27ME3	0.38	0.008
BENPORATH_EED_TARGETS	0.31	0.006
BRUINS_UVC_RESPONSE_VIA_TP53_GROUP_A	0.36	0
BENPORATH_SUZ12_TARGETS	0.24	0
BENPORATH_PRC2_TARGETS	0.28	0.04

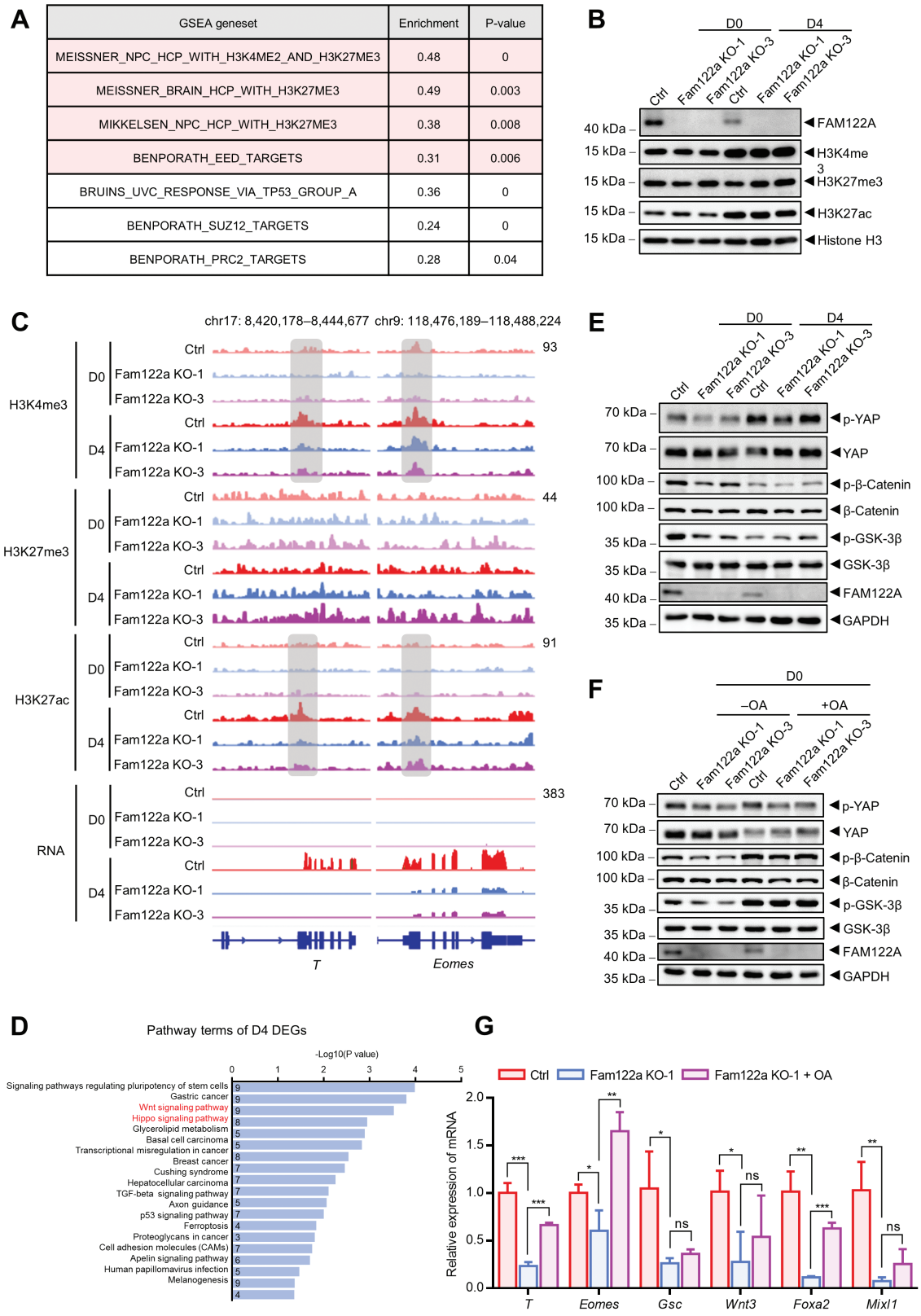

Figure 4. Wnt and Hippo signalings as well as histone modification dysregulated in *Fam122a* knockout mESCs. (**A**) GSEA of D0 Fam122a KO-1 DEGs. Gene sets changed in both KO mESCs are colored in red background (for color figure refer to online version). (**B**) Western blot analysis of histone modification proteins in D0 and D4 control and *Fam122a* knockout mESCs. (**C**) Genome browser views of H3K4me3, H3K27me3, and H3K27ac ChIP-seq signals as well as RNA expression in D0 and D4 indicated mESCs at mesendodermal genes *T* and *Eomes*. (**D**) KEGG pathway analysis of D4 DEGs. Numbers in bars show the gene numbers of the corresponding pathway categories. (**E**) Western blot analysis of p-YAP, p-β-catenin, and p-GSK-3β in D0 and D4 mESCs. (**F**) Western blot analysis of p-YAP, p-β-catenin, and p-GSK-3β in D0 indicated mESCs treated with or without 50 nM OA for 6 h. (**G**) qRT-PCR analysis of mesendodermal genes in D4 control and *Fam122a* KO EBs treated with or without 20 nM OA for the first 2 days. Data represent means ± SD from $n = 3$ independent experiments, and P values were calculated by 2-tailed unpaired t test (* $P < .05$, ** $P < .01$, and *** $P < .001$).

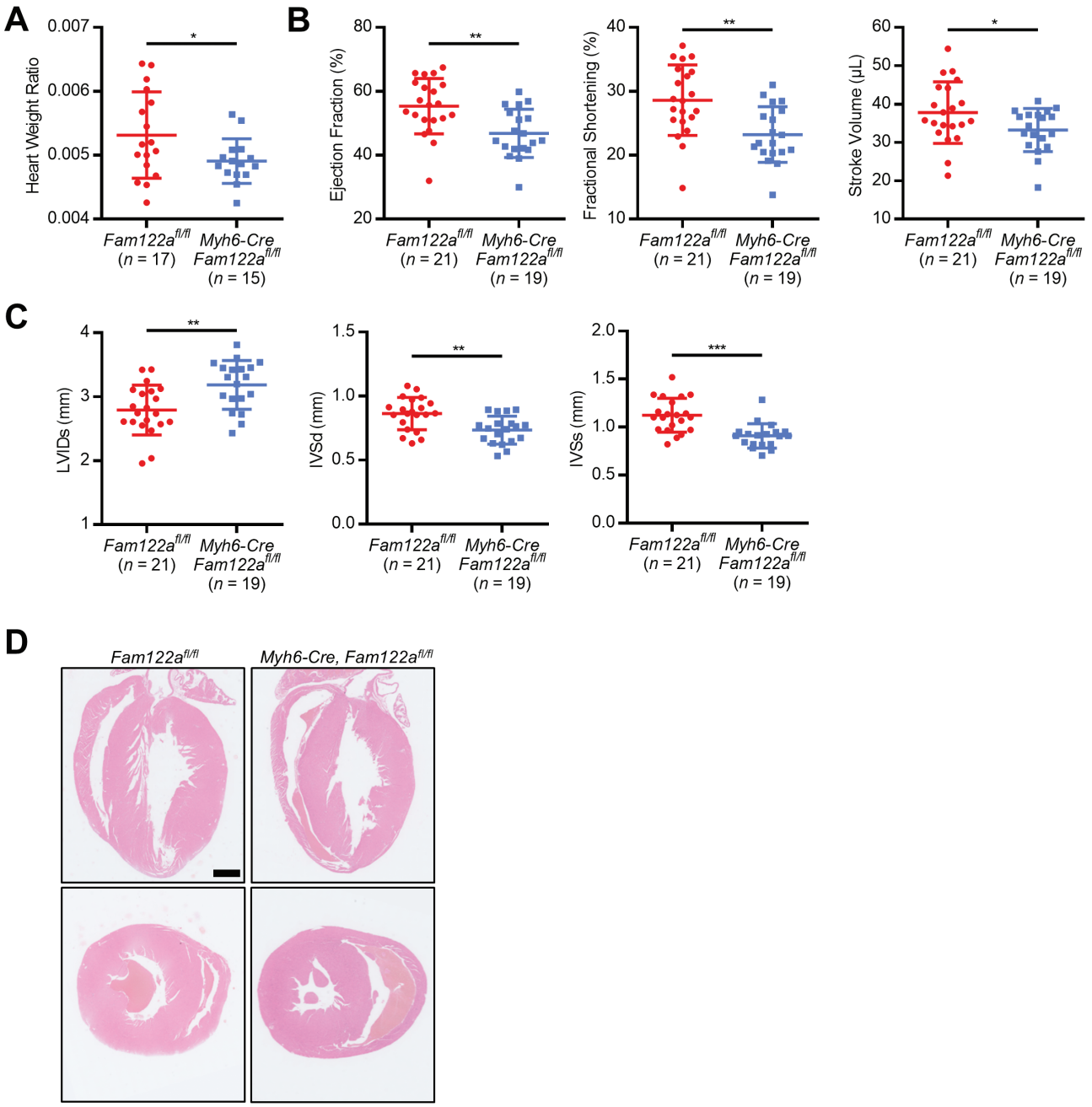

Figure 5. Cardiac function attenuated in *Myh6-Cre Fam122a* CKO mice. (**A**) Heart weight ratio analysis in *Fam122a*$^{flox/flox}$ (n = 17) and *Fam122a* CKO (n = 15) mice. (**B**) Echocardiography analyses for the EF, FS, and SV in *Fam122a*$^{flox/flox}$ (n = 21) and *Fam122a* CKO (n = 19) mice. (**C**) Echocardiography analyses for the LVID and IVS in diastole or systole in *Fam122a*$^{flox/flox}$ (n = 21) and *Fam122a* CKO (n = 19) mice. (**D**) H&E-stained sagittal or transverse sections of heart in *Fam122a*$^{flox/flox}$ and *Fam122a* CKO mice. Scale bar = 1 mm. In (A), (B), and (C), data represent means ± SD and P values were calculated by 2-tailed unpaired t test (* $P < .05$, ** $P < .01$, and *** $P < .001$).

Therefore, studies should find new target molecules in the regulation or manipulation of ES cells differentiating into ME, followed stepwise by differentiation into CMs. In our study, we have shown that FAM122A is critical for ME specification and CM differentiation from mESC in vitro culture system, as demonstrated by *Fam122a* deletion not only significantly impairing the expressions of MEPC-, CPC-, and CM-related genes but also reducing the percentages of spontaneously contracting EBs and Flk1^{+}/Pdgfra^{+} cardiac progenitors and TNNT2 protein. However, *Fam122a* deletion does not influence the stem cell identity.

The role of FAM122A in vivo study showed that *Fam122a* deletion led to early embryonic lethality with significantly severe defects in the cardiovascular system, including the deficiency in the normal structure of 4-chamber embryonic heart on E9.5 shown by HE staining and pericardial bulge revealed by anatomic microscopy. This finding supports the essential role of FAM122A in early embryonic and heart development. Two-conditional cardiac-specific *Fam122a* KO mice also displayed abnormal heart development and functions, as demonstrated by the decrease in cardiac functional indexes (EF, FS, and SV) and heart/weight ratio and altered structural

parameters (LVIDs, IVSd, and IVSs). However, these conditional *Fam122a* KO mice did not reproduce severe defects of heart development and embryonic lethality, which occurred in total *Fam122a* KO mice. Noticeably, the specific depletion of *Fam122a* in cardiac progenitors by Nkx2-5-Cre on E7.5 did not reveal striking cardiac defects, which suggests that FAM122A may affect considerably earlier developmental stages, such as ME, the dysfunction of which may further disrupt cardiac development and cardiomyocytic differentiation. Therefore, ME-specific Cre mice, such as Mesp1-Cre, or other ME drivers (Brachyury or Mixl1) may be used to further investigate the in vivo effect of *Fam122a* deletion on ME specification and confirm whether the in vivo effect is similar to the in vitro effect in mESCs (loss of ME gene expression upon *Fam122a* depletion). Considering that nascent mesoderm toward cardiac fates also relies on the signaling from proper endoderm development,[59] the effect of endodermal Cre (Foxa2 or Gsc)–driven deletion of *Fam122a* must be examined to exclude the possibility of cardiac defects upon *Fam122a* deletion resulting from impaired signaling from the overlaying foregut endoderm. These animal model should be analyzed in the future to confirm whether ME specification is disrupted upon *Fam122a* KO in vivo.

Currently, the understanding of the regulation networks of ME specification is limited, and its dynamic alteration is largely unclear. ME formation is highly organized and spatiotemporally controlled via the integrated interactions of TFs, epigenetic regulators, chromatin remodeling factors, and signaling pathways.[5,7] Substantial ME genes are suppressed upon *Fam122a* deletion, which includes the essential T-box TFs (*Eomes* and *T*) for ME differentiation. The GSEA dataset from DEGs in D4 EBs suggests that *Fam122a* deletion may affect histone modification of H3K4me2 and H3K27me3, which are closely related to ME specification.[60,61] ChIP-seq data regarding several histone modifications showed that *Fam122a* deletion decreased H3K4me3 binding on D0 and increased H3K27me3 binding in D4 EBs in a genome-wide manner, whereas no significant alteration was observed in H3K27ac. The altered histone modification pattern was accompanied by the upregulation of H3K27me3 protein in D4 EBs, which implies that FAM122A may regulate histone modification markers with different patterns before and after ME. More importantly, *Fam122a* depletion significantly decreased the association of H3K4me3 and H3K27ac with the promoters of *T* and *Eomes* genes in D4 EBs, which is consistent with the inhibitory effect of ME differentiation upon *Fam122a* depletion. However, IP-MS results depicted that no histone post-translational modifier interacted with FAM122A, which suggests that FAM122A may indirectly modulate histone modification by other unidentified mechanism or signaling pathway. In general, a default path of ectoderm differentiation exists when ME differentiation is absent[10]; however, our results suggest that *Fam122a* deletion may upregulate or downregulate ectoderm genes, and therefore, FAM122A participates in the regulation of ectoderm genes with a complexed mechanism.

FAM122A has no classical DNA binding motif and did not directly bind to the promoters of *Eomes* or *T* examined by ChIP-seq with Flag-FAM122A mESCs (data not shown), which suggests that FAM122A may modulate the expression of ME genes as a co-regulator or by influencing the chromatin structure. To address this question, scientists may apply ATAC-seq[62] to elucidate the effect of FAM122A modulation on chromatin architecture directly. Previously, we observed that FAM122A acts as a co-repressor of GATA-1 (an essential TF for erythroid differentiation) to suppress the terminal differentiation of erythroids[25]; therefore, FAM122A possibly interacts with essential ME-related TFs to participate in the regulation of ME gene activation, which needs to be checked dynamically in different stages of differentiation with IP-MS.

Mounting pieces of evidence show that TGF-β and Wnt signaling are critical for ME specification, and Wnt/Hippo signals are involved in the regulation of histone modification. Our results showed that DEGs between Fam122a KO and WT in D4 EBs are enriched in Wnt and Hippo signaling. YAP, an essential effector in Hippo signaling, has been recently reported to act as a negative regulator of ME differentiation. We observed that *Fam122a* deletion significantly decreased the phosphorylation levels of GSK-3β, β-catenin, and YAP, which suggests that *Fam122a* silencing dysregulates Wnt and YAP signaling pathways, thus affecting histone modification and impairing ME specification. OA can eliminate Fam122a KO–reduced phosphorylation of GSK-3β, β-Catenin, and YAP proteins, but it partially reverses the decreased effect of ME gene expression by *Fam122a* deletion, which strongly suggests that FAM122A regulates ME differentiation as a PP2A inhibitor. Zheng et al have identified a new dual-enzyme complex called INTAC for transcription regulation, and it is composed of PP2A core enzyme and multisubunit RNA endonuclease integrator.[63] In their model, PP2A dephosphorylates the C-terminal domain of RNA polymerase II to attenuate transcription. Therefore, whether FAM122A modulates ME gene expression through PP2A and/or INTAC warrants investigation.

Conclusion

Collectively, the results reveal that FAM122A, as possible PP2A inhibitor, is a critical regulator for ME specification and CM differentiation from mESCs through the dysregulation of histone modification and Wnt and Hippo signaling pathways. Moreover, *Fam122a* deletion leads to embryonic lethality with severe cardiovascular developmental defects and impairs cardiac function. The potential effects of FAM122A on stem cell differentiation into CMs not only provide new insights into its role in the development of 3-germ layers but can also contribute to clinical/therapeutic advancement in cardiac regenerative medicine in the future.

Acknowledgments

We thank Shanghai Frontiers Science Center of Cellular Homeostasis and Human Diseases for providing the experimental platforms and instruments.

Funding

This study was supported by the grant from Chinese National Natural Science Foundation (32070720, 82270244, H.Y.), Shanghai Jiao-Tong University, Research Units of Stress and Tumor (2019RU043, C.G.Q.), and Chinese Academy of Medical Sciences.

Conflict of Interest

The authors declare no potential conflicts of interests.

Author Contributions

Y.Y.: conception and design, collection and assembly of data, data analysis and interpretation, manuscript writing; M.L.: provision of study material; Z.Y.: collection of data; G.C.: final revision and approval of manuscript; Y.H.: conception and design, administrative support, manuscript writing, final approval of manuscript.

Data Availability

All data needed to evaluate the conclusions in the paper are present in the paper and/or Supplementary Materials. Additional data related to this paper may be requested from the authors.

Supplementary Material

Supplementary material is available at *Stem Cells* online.

References

1. Santini MP, Forte E, Harvey RP, Kovacic JC. Developmental origin and lineage plasticity of endogenous cardiac stem cells. *Development*. 2016;143(8):1242-1258. https://doi.org/10.1242/dev.111591
2. Savolainen SM, Foley JF, Elmore SA. Histology atlas of the developing mouse heart with emphasis on E11.5 to E18.5. *Toxicol Pathol*. 2009;37(4):395-414. https://doi.org/10.1177/0192623309335060
3. Sivakumar A, Kurpios NA. Transcriptional regulation of cell shape during organ morphogenesis. *J Cell Biol*. 2018;217(9):2987-3005. https://doi.org/10.1083/jcb.201612115
4. Tada S, Era T, Furusawa C, et al. Characterization of mesendoderm: a diverging point of the definitive endoderm and mesoderm in embryonic stem cell differentiation culture. *Development*. 2005;132(19):4363-4374. https://doi.org/10.1242/dev.02005
5. Wang L, Chen YG. Signaling control of differentiation of embryonic stem cells toward mesendoderm. *J Mol Biol*. 2016;428(7):1409-1422. https://doi.org/10.1016/j.jmb.2015.06.013
6. Alexanian M, Maric D, Jenkinson SP, et al. A transcribed enhancer dictates mesendoderm specification in pluripotency. *Nat Commun*. 2017;8(1):1806. https://doi.org/10.1038/s41467-017-01804-w
7. Jansen C, Paraiso KD, Zhou JJ, et al. Uncovering the mesendoderm gene regulatory network through multi-omic data integration. *Cell Rep*. 2022;38(7):110364. https://doi.org/10.1016/j.celrep.2022.110364
8. Beddington RS, Rashbass P, Wilson V. Brachyury—a gene affecting mouse gastrulation and early organogenesis. *Dev Suppl*. 1992;116(Supplement):157-165. https://doi.org/10.1242/dev.116.Supplement.157
9. Wilson V, Manson L, Skarnes WC, Beddington RS. The T gene is necessary for normal mesodermal morphogenetic cell movements during gastrulation. *Development*. 1995;121(3):877-886. https://doi.org/10.1242/dev.121.3.877
10. Tosic J, Kim GJ, Pavlovic M, et al. Eomes and Brachyury control pluripotency exit and germ-layer segregation by changing the chromatin state. *Nat Cell Biol*. 2019;21(12):1518-1531. https://doi.org/10.1038/s41556-019-0423-1
11. Costello I, Pimeisl IM, Dräger S, et al. The T-box transcription factor Eomesodermin acts upstream of Mesp1 to specify cardiac mesoderm during mouse gastrulation. *Nat Cell Biol*. 2011;13(9):1084-1091. https://doi.org/10.1038/ncb2304
12. Wang Q, Zou Y, Nowotschin S, et al. The p53 family coordinates Wnt and nodal inputs in mesendodermal differentiation of embryonic stem cells. *Cell Stem Cell*. 2017;20(1):70-86. https://doi.org/10.1016/j.stem.2016.10.002
13. Zhao M, Tang Y, Zhou Y, Zhang J. Deciphering role of Wnt signalling in cardiac mesoderm and cardiomyocyte differentiation from human iPSCs: four-dimensional control of Wnt pathway for hiPSC-CMs differentiation. *Sci Rep*. 2019;9(1):19389. https://doi.org/10.1038/s41598-019-55620-x
14. Brennan J, Lu CC, Norris DP, et al. Nodal signalling in the epiblast patterns the early mouse embryo. *Nature*. 2001;411(6840):965-969. https://doi.org/10.1038/35082103
15. Pauklin S, Vallier L. Activin/Nodal signalling in stem cells. *Development*. 2015;142(4):607-619. https://doi.org/10.1242/dev.091769
16. Nostro MC, Cheng X, Keller GM, Gadue P. Wnt, activin, and BMP signaling regulate distinct stages in the developmental pathway from embryonic stem cells to blood. *Cell Stem Cell*. 2008;2(1):60-71. https://doi.org/10.1016/j.stem.2007.10.011
17. Estaras C, Hsu HT, Huang L, Jones KA. YAP repression of the WNT3 gene controls hESC differentiation along the cardiac mesoderm lineage. *Genes Dev*. 2017;31(22):2250-2263. https://doi.org/10.1101/gad.307512.117
18. Zhou Q, Li L, Zhao B, Guan KL. The hippo pathway in heart development, regeneration, and diseases. *Circ Res*. 2015;116(8):1431-1447. https://doi.org/10.1161/CIRCRESAHA.116.303311
19. Fan L, Liu MH, Guo M, et al. FAM122A, a new endogenous inhibitor of protein phosphatase 2A. *Oncotarget*. 2016;7(39):63887-63900. https://doi.org/10.18632/oncotarget.11698
20. Fan F, Zhao J, Liu Y, et al. Identifying the SUMO1 modification of FAM122A leading to the degradation of PP2A-Calpha by ubiquitin-proteasome system. *Biochem Biophys Res Commun*. 2018;500(3):676-681. https://doi.org/10.1016/j.bbrc.2018.04.135
21. Li F, Kozono D, Deraska P, et al. CHK1 inhibitor blocks phosphorylation of FAM122A and promotes replication stress. *Mol Cell*. 2020;80(3):410-422.e6. https://doi.org/10.1016/j.molcel.2020.10.008
22. Zhou Y, Shi WY, He W, et al. FAM122A supports the growth of hepatocellular carcinoma cells and its deletion enhances Doxorubicin-induced cytotoxicity. *Exp Cell Res*. 2020;387(1):111714. https://doi.org/10.1016/j.yexcr.2019.111714
23. Liu MH, Chen J, Yang YS, et al. FAM122A promotes acute myeloid leukemia cell growth through inhibiting PP2A activity and sustaining MYC expression. *Haematologica*. 2021;106(3):903-907. https://doi.org/10.3324/haematol.2020.251462
24. Liu MH, Zhang XC, Chen J, et al. FAM122A is required for hematopoietic stem cell function. *Leukemia*. 2021;35(7):2130-2134. https://doi.org/10.1038/s41375-020-01099-9
25. Chen J, Zhou Q, Liu MH, et al. FAM122A inhibits erythroid differentiation through GATA1. *Stem Cell Rep*. 2020;15(3):721-734. https://doi.org/10.1016/j.stemcr.2020.07.010
26. Wang YQ, Yang YS, Chen J, et al. FAM122A maintains DNA stability possibly through the regulation of topoisomerase IIalpha expression. *Exp Cell Res*. 2020;396(1):112242. https://doi.org/10.1016/j.yexcr.2020.112242
27. Wei Q, Manley NR, Condie BG. Whole mount in situ hybridization of E8.5 to E11.5 mouse embryos. *J Vis Exp*. 2011;(56):e2797. https://doi.org/10.3791/2797
28. Guo X, Xu Y, Wang Z, et al. A Linc1405/Eomes complex promotes cardiac mesoderm specification and cardiogenesis. *Cell Stem Cell*. 2018;22(6):893-908.e6. https://doi.org/10.1016/j.stem.2018.04.013.
29. Wobus AM, Guan K, Yang HT, Boheler KR. Embryonic stem cells as a model to study cardiac, skeletal muscle, and vascular smooth muscle cell differentiation. *Methods Mol Biol*. 2002;185:127-156. https://doi.org/10.1385/1-59259-241-4:127
30. Dobin A, Davis CA, Schlesinger F, et al. STAR: ultrafast universal RNA-seq aligner. *Bioinformatics*. 2013;29(1):15-21. https://doi.org/10.1093/bioinformatics/bts635

31. Anders S, Pyl PT, Huber W. HTSeq-a Python framework to work with high-throughput sequencing data. *Bioinformatics*. 2015;31(2):166-169. https://doi.org/10.1093/bioinformatics/btu638
32. Love MI, Huber W, Anders S. Moderated estimation of fold change and dispersion for RNA-seq data with DESeq2. *Genome Biol*. 2014;15(12):550. https://doi.org/10.1186/s13059-014-0550-8
33. Langmead B, Salzberg SL. Fast gapped-read alignment with Bowtie 2. *Nat Methods*. 2012;9(4):357-359. https://doi.org/10.1038/nmeth.1923.
34. Tarasov A, Vilella AJ, Cuppen E, Nijman IJ, Prins P. Sambamba: fast processing of NGS alignment formats. *Bioinformatics*. 2015;31(12):2032-2034. https://doi.org/10.1093/bioinformatics/btv098
35. Ramirez F, Ryan DP, Grüning B, et al. deepTools2: a next generation web server for deep-sequencing data analysis. *Nucleic Acids Res*. 2016;44(W1);W160-165. https://doi.org/10.1093/nar/gkw257
36. Thorvaldsdottir H, Robinson JT, Mesirov JP. Integrative genomics viewer (IGV): high-performance genomics data visualization and exploration. *Brief Bioinform*. 2013;14(2):178-192. https://doi.org/10.1093/bib/bbs017
37. Farah CS, Reinach FC. The troponin complex and regulation of muscle contraction. *FASEB J*. 1995;9(9):755-767. https://doi.org/10.1096/fasebj.9.9.7601340
38. Barreto S, Hamel L, Schiatti T, Yang Y, George V. Cardiac progenitor cells from stem cells: learning from genetics and biomaterials. *Cells*. 2019;8(12):1536. https://doi.org/10.3390/cells8121536
39. Stefkova K, Prochazkova J, Pachernik J. Alkaline phosphatase in stem cells. *Stem Cells Int*. 2015;2015:628368. https://doi.org/10.1155/2015/628368
40. Hart AH, Hartley L, Sourris K, et al. Mixl1 is required for axial mesendoderm morphogenesis and patterning in the murine embryo. *Development*. 2002;129(15):3597-3608. https://doi.org/10.1242/dev.129.15.3597
41. Hong SP, Song S, Cho SW, et al. Generation of PDGFRalpha(+) cardioblasts from pluripotent stem cells. *Sci Rep*. 2017;7(1):41840. https://doi.org/10.1038/srep41840
42. Chen CY, Cheng YY, Yen CY, Hsieh PC. Mechanisms of pluripotency maintenance in mouse embryonic stem cells. *Cell Mol Life Sci*. 2017;74(10):1805-1817. https://doi.org/10.1007/s00018-016-2438-0
43. Sharma A, Mir R, Galande S. Epigenetic regulation of the Wnt/beta-catenin signaling pathway in cancer. *Front Genet*. 2021;12:681053. https://doi.org/10.3389/fgene.2021.681053
44. Liu X, Li Z, Song Y, et al. AURKA induces EMT by regulating histone modification through Wnt/beta-catenin and PI3K/Akt signaling pathway in gastric cancer. *Oncotarget*. 2016;7(22):33152-331643. https://doi.org/10.18632/oncotarget.8888
45. Oh H, Slattery M, Ma L, et al. Yorkie promotes transcription by recruiting a histone methyltransferase complex. *Cell Rep*. 2014;8(2):449-459. https://doi.org/10.1016/j.celrep.2014.06.017
46. Qing Y, Yin F, Wang W, et al. The Hippo effector Yorkie activates transcription by interacting with a histone methyltransferase complex through Ncoa6. *Elife*. 2014;3:e02564. https://doi.org/10.7554/eLife.02564
47. Arkell RM, Fossat N, Tam PP. Wnt signalling in mouse gastrulation and anterior development: new players in the pathway and signal output. *Curr Opin Genet Dev*. 2013;23(4):454-460. https://doi.org/10.1016/j.gde.2013.03.001
48. Mia MM, Singh MK. The hippo signaling pathway in cardiac development and diseases. *Front Cell Dev Biol*. 2019;7:211. https://doi.org/10.3389/fcell.2019.00211
49. Jiang X, Hu J, Wu Z, et al. Protein phosphatase 2A mediates YAP activation in endothelial cells upon VEGF stimulation and matrix stiffness. *Front Cell Dev Biol*. 2021;9:675562. https://doi.org/ARTN 67556210.3389/fcell.2021.675562
50. Brewer CM, Nelson BR, Wakenight P, et al. Adaptations in Hippo-Yap signaling and myofibroblast fate underlie scar-free ear appendage wound healing in spiny mice. *Dev Cell*. 2021;56(19):2722-2740.e2726. https://doi.org/10.1016/j.devcel.2021.09.008
51. Xiao Z, Wen L, Zeng D, et al. Protein phosphatase 2A inhibiting beta-catenin phosphorylation contributes critically to the anti-renal interstitial fibrotic effect of norcantharidin. *Inflammation*. 2020;43(3):878-891. https://doi.org/10.1007/s10753-019-01173-0
52. Wu MY, Xie X, Xu ZK, et al. PP2A inhibitors suppress migration and growth of PANC-1 pancreatic cancer cells through inhibition on the Wnt/beta-catenin pathway by phosphorylation and degradation of beta-catenin. *Oncol Rep*. 2014;32(2):513-522. https://doi.org/10.3892/or.2014.3266
53. Chu DD, Tan J, Xie S, et al. GSK-3 beta is dephosphorylated by PP2A in a Leu309 methylation-independent manner. *J Alzheimers Dis*. 2016;49(2):365-375. https://doi.org/10.3233/Jad-150497
54. Mitra A, Menezes ME, Pannell LK, et al. DNAJB6 chaperones PP2A mediated dephosphorylation of GSK3beta to downregulate beta-catenin transcription target, osteopontin. *Oncogene*. 2012;31(41):4472-4483. https://doi.org/10.1038/onc.2011.62
55. Huang X, Yan L, Kou S, et al. Generation and characterization of a Myh6-driven Cre knockin mouse line. *Transgenic Res*. 2021;30(6):821-835. https://doi.org/10.1007/s11248-021-00285-4
56. Moses KA, DeMayo F, Braun RM, Reecy JL, Schwartz RJ. Embryonic expression of an Nkx2-5/Cre gene using ROSA26 reporter mice. *Genesis*. 2001;31(4):176-180. https://doi.org/10.1002/gene.10022
57. Bertero A, Murry CE. Hallmarks of cardiac regeneration. *Nat Rev Cardiol*. 2018;15(10):579-580. https://doi.org/10.1038/s41569-018-0079-8
58. Choi WY, Poss KD. Cardiac regeneration. *Curr Top Dev Biol*. 2012;100:319-344. https://doi.org/10.1016/B978-0-12-387786-4.00010-5
59. Zhang L, Nomura-Kitabayashi A, Sultana N, et al. Mesodermal Nkx2.5 is necessary and sufficient for early second heart field development. *Dev Biol*. 2014;390(1):68-79. https://doi.org/10.1016/j.ydbio.2014.02.023
60. Xie W, Schultz MD, Lister R, et al. Epigenomic analysis of multilineage differentiation of human embryonic stem cells. *Cell*. 2013;153(5):1134-1148. https://doi.org/10.1016/j.cell.2013.04.022
61. Xie R, Everett LJ, Lim HW, et al. Dynamic chromatin remodeling mediated by polycomb proteins orchestrates pancreatic differentiation of human embryonic stem cells. *Cell Stem Cell*. 2013;12(2):224-237. https://doi.org/10.1016/j.stem.2012.11.023
62. Sun Y, Miao N, Sun T. Detect accessible chromatin using ATAC-sequencing, from principle to applications. *Hereditas*. 2019;156(1):29. https://doi.org/10.1186/s41065-019-0105-9
63. Zheng H, Qi Y, Hu S, et al. Identification of Integrator-PP2A complex (INTAC), an RNA polymerase II phosphatase. *Science*. 2020;370(6520):eabb5872. https://doi.org/10.1126/science.abb5872